Multilayer buffer for high-temperature superconductor devices on MgO

M. I. Faley,[a] S. B. Mi, A. Petraru, C. L. Jia, U. Poppe, and K. Urban
IFF, Forschungszentrum Jülich GmbH, D-52425 Jülich, Germany

(Received 17 May 2006; accepted 17 July 2006; published online 22 August 2006)

A multilayer thin film epitaxial passivation of single crystal MgO substrates was developed. $YBa_2Cu_3O_{7-x}$ films on the buffered MgO substrates demonstrate pure *c*-axis orientation, absence of in-plane disoriented grains, transition temperature $T_c > 91$ K, and critical current density $J_c \sim 5$ MA/cm^2 at 77.4 K and were deposited in thicknesses of up to several micrometers without cracks. High-temperature superconductor multilayer flux transformers of 2 μm thickness on the buffered MgO substrates demonstrated improved insulation between the superconducting layers and an increased dynamic range compared to flux transformers on $SrTiO_3$ substrates. © *2006 American Institute of Physics*. [DOI: 10.1063/1.2338564]

The preparation of epitaxial films of high-temperature superconductor (HTS) $YBa_2Cu_3O_{7-x}$ (YBCO) and many other oxide materials is performed at substrate temperatures of 700–900 °C higher than their storage and operation temperatures. The difference in the thermal expansion coefficients of the oxide materials used for the substrates and films leads to a tensile strain in the YBCO films which degrades their superconducting properties and can even crack the films when their thickness exceeds some critical value. Thick multilayer HTS thin film structures such as multiturn flux transformers are, for example, required for the production of sensitive superconducting quantum interference device (SQUID) magnetometers.[1] The high critical current of the HTS films is also beneficial for high-*Q* microwave resonators and filters used in communication technologies as well as for HTS tapes intended for the generation and transport of electrical power applications.

MgO substrates have similar thermal expansion coefficients to that of YBCO. The main disadvantage of MgO substrates is the degradation of the hygroscopic surface in the air. These substrates also have a lattice mismatch of ~9% with YBCO and a different crystal structure. These properties usually lead to a significant amount of in-plane 45° misoriented grains in the YBCO films deposited on MgO substrates, which significantly suppresses the average critical current density of the HTS films.[2] Surface treatment methods such as annealing at temperatures of ~1100 °C or ion beam etching of the substrate surface as well as deposition of buffer layer materials such as $SrTiO_3$ (STO) or $BaZrO_3$ (BZO) have been suggested in order to improve the epitaxial growth of YBCO films on MgO substrates.[2–4] The buffer preserved the hygroscopic surface of the MgO substrates from degradation in air and/or during the lithographic procedures. At least two buffer layers are required to deposit YBCO on MgO: the first one should provide the epitaxial growth of films with perovskite structure on the rocksalt structure of MgO, while the second buffer layer should match the lattice constants.[4]

In the present letter we describe a multilayer thin film buffer which provided an epitaxial passivation of the surface of the single crystal MgO substrates and allowed a significant improvement of the epitaxial growth of the relatively thick crack-free YBCO films on it. The buffer technology thus developed can be used to prepare high-I_c and/or low-noise multilayer HTS thin film devices as well as for other applications of the oxide films such as the high density ferroelectric memory cells.[5]

High-oxygen-pressure sputtering[6] was used to deposit the thin film buffer layers and YBCO films on STO, $LaAlO_3$ (LAO), $NdGaO_3$ (NGO), and MgO single crystal substrates. A single crystal STO wafer was used as a target while BZO, YBCO, and $PrBa_2Cu_3O_{7-x}$ (PBCO) targets were polycrystalline. The deposition rate of the YBCO and PBCO films was ~50 nm/h while the deposition rate of the nonconducting materials was ~10 nm/h. During deposition the substrates were positioned freely on the heater with temperatures of up to ~1000 °C, which corresponded to a substrate temperature of ~850 °C. The BZO, STO, YBCO, and PBCO films were deposited in an atmosphere of pure (99.999%) oxygen at pressures of ~3 mbar, which at the substrate temperature of ~850 °C corresponded to the Hammond-Bormann ($CuO–Cu_2O–O_2$) line[7] for optimal deposition of YBCO films. The deposition conditions and microstructural properties of the STO films were similar to ones described earlier.[8] We have observed that the epitaxial STO buffer layer significantly improved the *c*-axis oriented epitaxial growth of YBCO and PBCO films on the STO, LAO, and NGO substrates.

The pristine MgO substrates were first investigated by atomic force microscope (AFM) to select the nondegraded substrates with a root-mean-square roughness of the surface <0.2 nm for further processing. Such control of the substrate surface was especially important for the MgO substrates, because some of them were transported and/or stored for a long time in air. The substrate surface should also be free from residuals of polishing abrasives such as silica (SiO_2), which can chemically react with MgO at high deposition temperatures creating the magnesium silicates, e.g., Mg_2SiO_4. No annealing and/or ion beam etching of the pristine substrates were applied because according to our experience these procedures often degrade the original morphology and crystalline microstructure of the substrate surfaces.

The epitaxial passivation of MgO substrates consisted of two buffer layers made of different compounds. The first 30-nm-thick BZO layer deposited served to change the crystal structure of the surface from the rocksalt to perovskite type. Above the BZO layer a 30- to 300-nm-thick STO layer was deposited to avoid formation of Ba_2ZrYO_6 (Ref. 8) and

[a]Electronic mail: m.faley@fz-juelich.de

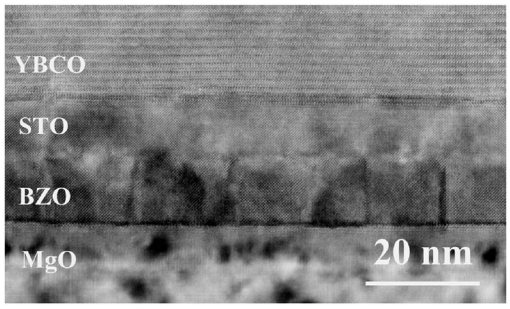

FIG. 1. Cross-sectional HRTEM image of a BZO–STO–YBCO heterostructure deposited on a MgO (100) substrate.

achieve a better matching of the lattice constant of the buffer with YBCO.

We established by AFM measurements that the multilayer epitaxial passivation with BZO–STO completely covered the surface of the MgO substrates and a root-mean-square roughness <0.2 nm was observed. A cross-sectional high resolution transmission electron microscopy (HRTEM) image of the BZO–STO–YBCO heterostructure deposited on a MgO (100) substrate is shown in Fig. 1. Columnlike growth of the BZO layer was stopped at the BZO–STO interface. The STO layer also significantly smoothed the ~ 1 nm roughness of the surface, which had appeared on the BZO layer. A STO layer thickness of ~ 10 nm was found to be sufficient for complete coverage of the substrate and epitaxial growth of the YBCO films on it. The thickness of the STO layer was increased up to ~ 300 nm without any increase of surface roughness or the appearance of cracks. Such a relatively thick buffer layer provided sufficient passivation of the MgO substrate surface for storage and lithography including patterning of the structures by ion beam milling.

In the plan view HRTEM image we observed Y_2O_3 inclusions, which were lattice-coherently integrated in the relatively unstrained crystal matrix of YBCO. According to our experience, the strain in the YBCO films deposited on LAO, NGO, and STO substrates was concentrated at such inclusions which thus served as the origins for microcracks in the films. In the case of MgO substrates, even an ~ 1 μm thickness of the YBCO film did not lead to any observable strain around the Y_2O_3 inclusions.

Crystal structure and orientation of the deposited oxide films were investigated by 2Θ and ϕ scans with x-ray diffraction (XRD). The XRD patterns (see Fig. 2) demonstrated a perfect *c*-axis and in-plane orientation of the YBCO film. The in-plane orientation of ~ 1-μm-thick YBCO films deposited on buffered MgO (100) substrate was checked by YBCO (103) XRD ϕ scans and plan view HRTEM. No misoriented grains were observed for the YBCO films deposited on freshly polished and/or buffered MgO substrates. Each of the four peaks in the YBCO (103) ϕ scan pattern was doubled due to the in-plane twin structure of the YBCO film. A (101) ϕ scan pattern with four unsplitted peaks of much smaller amplitude at the same positions was observed for buffer layers. Fortunately for the MgO substrate (101) ϕ scan peaks are forbidden and were not registered.

In the case of unbuffered MgO substrates exposed for a long time to air the ϕ scan pattern of the YBCO film contained four additional peaks, corresponding to the presence of the 45° in-plane misoriented grains. The amplitudes of these peaks increased with the exposure time corresponding to an increased number of 45° misoriented grains. The epitaxial multilayer buffer described here prevented the surface of the MgO substrates from such degradation.

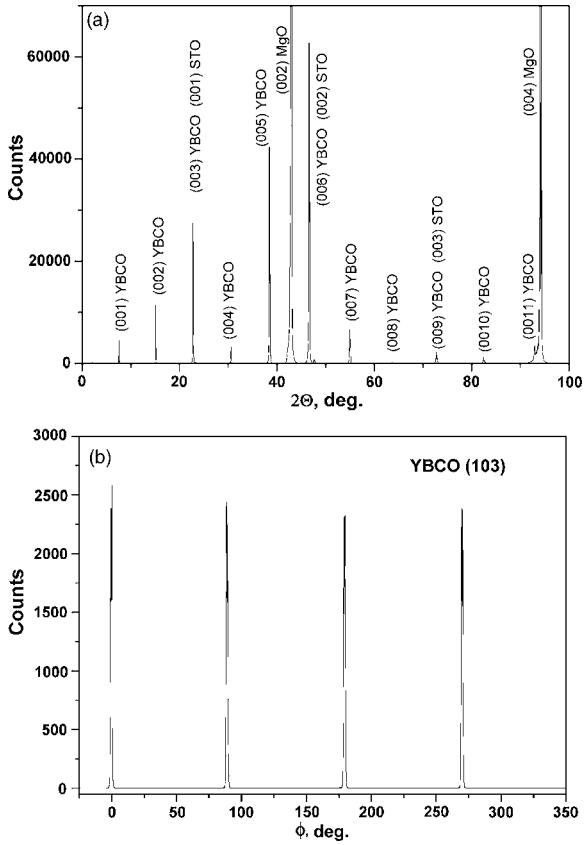

FIG. 2. XRD (a) Θ-2Θ scan and (b) ϕ scan for an ~ 1-μm-thick YBCO film deposited on a buffered MgO (100) substrate.

The use of a buffer layer also helped improve the morphology of the YBCO film surface. Pure *c*-axis oriented YBCO films were obtained on buffered MgO substrates at substrate temperatures between 650 and 850 °C. The density of growth spirals decreased with temperature from $\sim 10^{10}$ cm^{-2} at a substrate temperature of ~ 650 °C down to $\sim 4\times 10^6$ cm^{-2} at a substrate temperature of ~ 850 °C. A relatively low density ($\sim 10^6$ cm^{-2}) of CuO precipitates and holes was observed. The diameters of the precipitates and holes were <1 μm even for the YBCO film thicknesses of ~ 2 μm. This allowed patterning of such films for a reproducible production of devices with structural widths of $\geqslant 1$ μm.

Cracks in the YBCO films were observed on all substrates except MgO (see Fig. 3). YBCO films of about ~ 1.7 μm in thickness were deposited on STO (100) substrates and on buffered MgO (100) substrates and then thinned by ion beam milling down to a thickness of ~ 100 nm to reveal possible internal cracks in the YBCO films. It was observed that the cracks for the LAO (100) and NGO (110) substrates started to appear on ~ 0.5-μm-thick YBCO films whereas for the STO substrates they appeared in the YBCO film at a thickness of ~ 1 μm. In the case of NGO (110) substrates, the observed cracks had a preferential orientation in the $[\bar{1}10]$ direction normal to the substrate $[001]$ *c* axis.

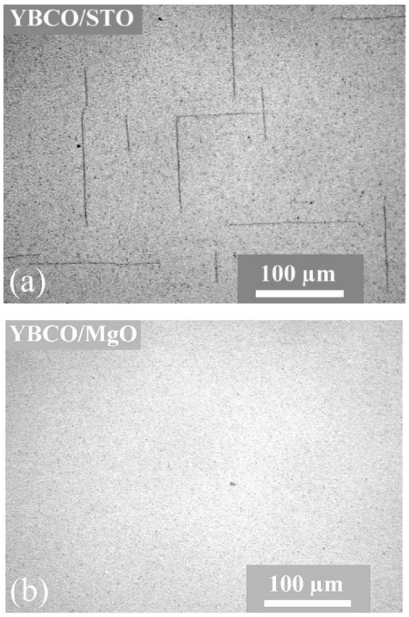

FIG. 3. Optical images of crack structures in YBCO films deposited under similar conditions on (a) $SrTiO_3$ (100) and (b) buffered MgO (100) substrates.

The YBCO films deposited on the buffered MgO substrates had typical critical current densities $J_c \sim 5 \times 10^6$ A/cm^2 at 77.4 K, and the superconducting transition temperature T_c exceeded 91 K. The thickness dependences of the room temperature effective resistivity of the YBCO films deposited at similar conditions on LAO, STO, and buffered MgO substrates are shown in Fig. 4. Only the YBCO films on buffered MgO substrates demonstrated conductivity proportional to the film thickness. The conductivity of YBCO films on other substrates saturated or even dropped when the thicknesses exceeded the critical values where cracks appeared in the films.

HTS Josephson junctions and direct coupled dc SQUIDs on the buffered MgO bicrystal substrates with a 24° in-plane misorientation angle were investigated at temperatures of 4.2–77.4 K. The critical current of the junctions I_c showed in the medium temperature range of 10–85 K an almost linear temperature dependence $I_c(T)/I_c(T=0) \sim (1\text{-}T/T_c)$ similar to one of the HTS bicrystal junctions on other substrates.

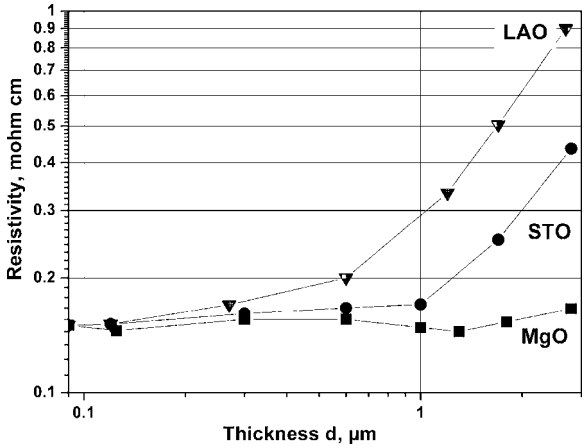

FIG. 4. Thickness dependence of the effective resistivity for YBCO films deposited under similar conditions on LAO (▼), STO (●), and buffered MgO (■) substrates.

I_cR_n products of ~300 μV at 77.4 K and ~2 mV at 4.2 K were achieved for the junctions. The junctions demonstrated hysteretic $I(V)$ characteristics at 4.2 K corresponding to a McCumber parameter $\beta_c = 2\pi I_c R_n^2 C/\Phi_0 > 1$. The capacitance C estimated from β_c for a 2×0.1 μm^2 bicrystal junction was ~30 fF. This value was in agreement with the results of Ref. 9 and was similar to the capacitance of the bicrystal junctions prepared on other substrate materials. The substrate contribution to the junction capacitance is much less compared to the contribution of the grain boundary capacitance because[10,11] at relevant β_c frequencies of ~750 GHz and temperatures of ~20 K the dielectric constant of STO is less than 100.

Direct coupled dc SQUIDs with a loop inductance of 100 pH produced on the buffered MgO substrates showed a flux resolution $\sim 15\mu\Phi_0/\sqrt{\text{Hz}}$ at 77.4 K, which is similar to the flux resolution of dc SQUIDs on STO substrates.[1] A further decrease of the temperature leads to an increase of the white noise due to the appearance of a hysteresis in the $I(V)$ characteristics of the junctions ($\beta_c > 1$).

We used buffered MgO substrates mainly for the preparation of multilayer flux transformers. Application of the buffered MgO substrates instead of the traditionally used STO substrates allowed us to increase the thickness of all layers in such a heterostructure containing two YBCO layers and one PBCO nonsuperconducting layer for about twofold up to a total thickness of ~2 μm. This helped us to improve the insulation between the superconducting layers and increase the critical current of the flux transformer. Thus the reproducibility and dynamic range of the flux transformers were significantly improved.

In conclusion, an epitaxial multilayer thin film buffer served for passivation of the single crystal MgO substrates to improve the epitaxial growth of the YBCO films. The multilayer buffer has preserved surface of the MgO substrate from degradation during patterning of the multilayer structures and devices.

The authors gratefully acknowledge useful discussions with Y. Divin and the technical assistance of R. Speen.

[1] M. I. Faley, U. Poppe, K. Urban, D. N. Paulson, T. Starr, and R. L. Fagaly, IEEE Trans. Appl. Supercond. **11**, 1383 (2001); M. I. Faley, U. Poppe, K. Urban, V. Yu. Slobodchikov, Yu. V. Maslennikov, A. Gapelyuk, B. Sawitzki, and A. Schirdewan, Appl. Phys. Lett. **81**, 2406 (2002).
[2] J. Du, S. Gnanarajan, and A. Bendavid, Supercond. Sci. Technol. **18**, 1035 (2005).
[3] A. Inoue, M. Kai, S. Hoshi, T. Izumi, Y. Shiohara, and K. Murata, Physica C **392–396**, 965 (2003).
[4] R. Hühne, D. Selbmann, J. Eickemeyer, J. Hänisch, and B. Holzapfel, Supercond. Sci. Technol. **19**, 169 (2006).
[5] *Polar Oxides: Properties, Characterization, and Imaging*, edited by R. Waser, U. Böttger, and S. Tiedke (Wiley-VCH, Weinheim, 2005).
[6] U. Poppe, N. Klein, U. Dähne, H. Soltner, C. L. Jia, B. Kabius, K. Urban, A. Lubig, K. Schmidt, S. Hensen, S. Orbach, G. Müller, and H. Piel, J. Appl. Phys. **71**, 5572 (1992).
[7] R. H. Hammond and R. Bormann, Physica C **162–164**, 703 (1989); R. Feenstra, T. B. Lindemer, J. D. Budai, and M. D. Galloway, J. Appl. Phys. **69**, 6569 (1991).
[8] M. I. Faley, C. L. Jia, U. Poppe, L. Houben, and K. Urban, Supercond. Sci. Technol. **19**, S195 (2006).
[9] J. L. Macmanus-Driscoll, S. R. Foltyn, Q. X. Jia, H. Wang, A. Serquis, L. Civale, B. Maiorov, M. E. Hawley, M. P. Maley, and D. E. Peterson, Nat. Mater. **3**, 439 (2004).
[10] P. F. McBrien, R. H. Handfield, W. E. Booij, A. Moya, F. Kahlmann, M. G. Blamire, C. M. Pegrum, E. J. Tarte, Physica C **339**, 88 (2000).
[11] P. Dore, G. De Marzi, and A. Paolone, Int. J. Theor. Phys. **18**, 125 (1997).